CALCIUM-ACTIVATED HYPERPOLARIZATIONS IN RAT LOCUS COERULEUS NEURONS *IN VITRO*

By SMAJO S. OSMANOVIĆ AND SARAH A. SHEFNER

From the Department of Physiology and Biophysics, University of Illinois at Chicago, College of Medicine, Chicago, IL 60612, USA

SUMMARY

1. Intracellular recordings were made from rat locus coeruleus (LC) neurons in completely submerged brain slices. Trains of action potentials in LC neurons were followed by a prolonged post-stimulus hyperpolarization (PSH). If trains were elicited with depolarizing current pulses of sufficient intensity, PSH was composed of a fast, early component (PSH_E) and a slow, late component (PSH_L). PSH which followed trains elicited with lower intensity depolarizing current pulses consisted only of PSH_L.

2. Both PSH_E and PSH_L were augmented by increasing the number of action potentials in the train and both were associated with an increase in membrane conductance. The reversal potential for PSH_E was -108 mV and for PSH_L it was -114 mV.

3. When a hybrid voltage clamp protocol was used, the current underlying PSH (I_{PSH}) was observed to consist of an early, rapidly decaying component, I_E, followed by a late, slower decaying component, I_L. The time course of decay of I_{PSH} was biexponential with the time constant of decay of I_L more than one order of magnitude larger than the time constant of decay of I_E. An increase in the concentration of external K^+ shifted the reversal potentials for I_E and I_L in the depolarizing direction; the mean value of shift per tenfold increase in external K^+ concentration was $57 \cdot 1$ mV for I_E and $57 \cdot 6$ mV for I_L.

4. Both PSH_E and PSH_L were inhibited by lowering the external Ca^{2+} concentration or by application of the Ca^{2+} channel blockers Cd^{2+} (200–500 μM) or nifedipine (100 μM). Intracellular injection of EGTA abolished both components of PSH. Increasing the external Ca^{2+} concentration augmented both PSH components.

5. Superfusion of dantrolene (25 μM) or ryanodine (20 μM) decreased the amplitude and duration of PSH_L with much less effect on PSH_E.

6. *d*-Tubocurarine (20–200 μM) selectively blocked PSH_E with no effect on PSH_L; this effect is the same as that of apamin which we have previously described. Superfusion with charybdotoxin (40 nM) or TEA (400 μM–1 mM) did not reduce PSH_E or PSH_L.

7. Inhibition of I_A by 4-aminopyridine or 2,4-diaminopyridine also did not reduce either component of PSH. In fact, these agents slightly augmented both components of PSH; this effect was probably secondary to the prolongation of action potential

duration. Superfusion of TEA in concentrations of 2–10 mM increased the size and duration of PSH_L and increased the duration but decreased the size of PSH_E.

8. Superfusion with noradrenaline (10 μM), dibutyryl cAMP or 8-Br-cAMP (1 mM) did not affect either component of PSH. Carbachol (40–100 μM) increased the size and duration of PSH_L without changing PSH_E.

9. The results indicate that PSH in LC neurones is mediated by two types of Ca^{2+}-dependent K^+ conductances with different time courses and pharmacological properties. The early component is selectively blocked by apamin and d-tubocurarine, while the late component is reduced by blockers of Ca^{2+}-induced Ca^{2+} release and enhanced by muscarinic agonists.

INTRODUCTION

Intense firing of locus coeruleus (LC) neurons is followed by a large hyperpolarization, which has been referred to as a long-lasting after-hyperpolarization (Andrade & Aghajanian, 1984), post-tetanic hyperpolarization (Williams, North, Shefner, Nishi & Egan, 1984) or post-stimulus hyperpolarization (Osmanović & Shefner, 1988). This hyperpolarization underlies the post-activation inhibition of firing in LC neurons observed *in vivo* following intracellular injection of depolarizing current (Aghajanian & VanderMaelen, 1982) or antidromic or orthodromic stimulation (Aghajanian, Cedarbaum & Wang, 1977; Watabe & Satoh, 1979). This phenomenon appears to be of physiological importance since noxious cutaneous stimulation *in vivo* also causes increased firing of LC neurons, followed by a prolonged quiescent period (Aghajanian, VanderMaelen & Andrade, 1983).

Several lines of evidence suggest that the post-stimulus hyperpolarization (PSH) in LC neurons is mediated by activation of a Ca^{2+}-activated K^+ conductance. Firstly, PSH is attenuated in Ca^{2+}-free media and by blockers of Ca^{2+} channels (Andrade & Aghajanian, 1984; Williams *et al.* 1984). In addition, intracellular injection of the Ca^{2+} chelator EGTA reduces PSH (Aghajanian *et al.* 1983). Finally, the reversal potential for PSH is close to the K^+ equilibrium potential and changes as a function of external K^+ concentration in the direction predicted by the Nernst equation (Andrade & Aghajanian, 1984; Williams *et al.* 1984).

Since these initial descriptions of PSH in LC neurons, numerous studies in other preparations have revealed the existence of several distinct types of Ca^{2+}-activated K^+ conductance, which differ in their Ca^{2+} and voltage dependence, their pharmacological properties, and their single channel conductances (see Rudy, 1988, for review). In this study, we have attempted to characterize the specific types of Ca^{2+}-activated K^+ conductance which mediate PSH in locus coeruleus neurons. A portion of this work has been reported previously in abstract form (Osmanović & Shefner, 1990*a*).

METHODS

Experiments were performed on rat locus coeruleus neurons in a brain slice preparation from male Sprague–Dawley and Fisher 344 rats (100–200 g). The preparation of rat pontine slices has been described in detail previously (Osmanović & Shefner, 1990*b*). Briefly, rats were killed by cervical dislocation and the brain rapidly removed. A block of tissue containing the pons was prepared and then submerged in cooled (4–6 °C) oxygenated artificial cerebrospinal fluid (ACSF)

in the well of a Lancer vibratome. A coronal slice (300 μm thick) which contained the caudal portion of LC was cut and mounted in the recording chamber (0·3 ml volume). Slices were completely submerged in ACSF of the following composition (mM): NaCl, 126; KCl, 2·5; MgSO$_4$, 1·3; CaCl$_2$, 2·4; NaH$_2$PO$_4$, 1·2; NaHCO$_3$, 26; glucose, 11 (saturated with 95% O$_2$–5% CO$_2$, pH 7·4). The temperature of the ACSF was 35·5–36·5 °C and the flow rate was 2·2 ml/min. Recording electrodes were placed in the LC under visual control; the LC nucleus can be identified in the living slice as a clearly defined, bright, translucent area when viewed with transmitted light. Intracellular recording electrodes were made on a Brown-Flaming puller from glass micropipettes (o.d. = 1·0 mm) and were filled with 2 M KCl. Electrodes were selected for use if they had DC resistances of 40–80 MΩ and were capable of passing a steady current of 1 nA. For intracellular injection of EGTA, recording pipettes were filled with EGTA dissolved in a solution of 4 M potassium acetate. There was no difference in PSH recorded with 4 M potassium acetate electrodes as compared to 2 M KCl-filled electrodes. Current-clamp recordings were obtained with an amplifier with active bridge circuit which allowed current injection through the recording electrode. The bridge balance was adjusted inside each cell as necessary, and checked during the experiment. In voltage-clamp experiments a single-electrode voltage-clamp circuit (Axoclamp 2A, Axon Instruments) was used. Input capacitance was minimized by careful selection of microelectrodes and keeping the level of ACSF in the chamber low. The switching frequency (3–4 kHz) and capacity compensation were adjusted in discontinuous current-clamp mode by monitoring the headstage voltage responses to current pulses. During each experiment, the headstage voltage was continually monitored on a separate oscilloscope to ensure that the voltage transients across the microelectrode decayed fully before voltage sampling. The resting membrane potential was determined at the end of each experiment after withdrawing the electrode from the cell.

PSH was elicited by trains of action potentials evoked by depolarizing current pulses applied through the recording electrode. The number of action potentials in the train used to evoke PSH was kept constant in control and after switching to ACSF containing drug or differing in ionic composition. In order to do this, the number of spikes in the train was adjusted by changing the duration of the current pulse, while keeping the stimulus intensity constant. This was done in order to avoid changes in the early component of PSH, as described in the results section, below.

Voltages and currents were displayed on a storage oscilloscope and Gould rectilinear pen-recorder. In most experiments, current and voltage data were digitized with an Instrutech VR-10 A/D converter and recorded on videotape for later analysis. Biexponential curves were fitted to the data by a computer program which applies the simplex algorithm for minimizing least-squares error. All quantitative data in the text are expressed as means ± S.E.M.

All drugs were purchased from Sigma USA, except charybdotoxin (Natural Products Sciences, Inc., Salt Lake City, UT, USA) and ryanodine (Research Biochemicals, Inc., Natick, MA, USA). Dantrolene was dissolved in dimethyl sulphoxide (DMSO) and ryanodine in methanol to make 25 mM stock solutions which were then diluted with ACSF to the final concentrations. The concentrations of DMSO and methanol present in these drug solutions (0·1%) were tested before drug addition, to control for any changes in PSH due to the vehicle. All other drugs were dissolved in ACSF; solutions were prepared just before use to ensure full potency. A valve system was used to switch superfusing solutions from control ACSF to ACSF containing drug or differing in ionic composition. Time to attain equilibration to full concentration of drug in the chamber was approximately 2 min. All drugs were administered for sufficient time to reach a steady-state response (2 min or longer). When ionic substitution or drug application caused a change in membrane potential, PSH amplitude and duration were always measured after the membrane potential was returned to control level by DC current injection.

RESULTS

Neurons selected for this study ($n = 86$) had stable resting membrane potentials of -57 to -64 mV, overshooting action potentials with amplitudes of more than 70 mV and input resistances of 180–320 MΩ.
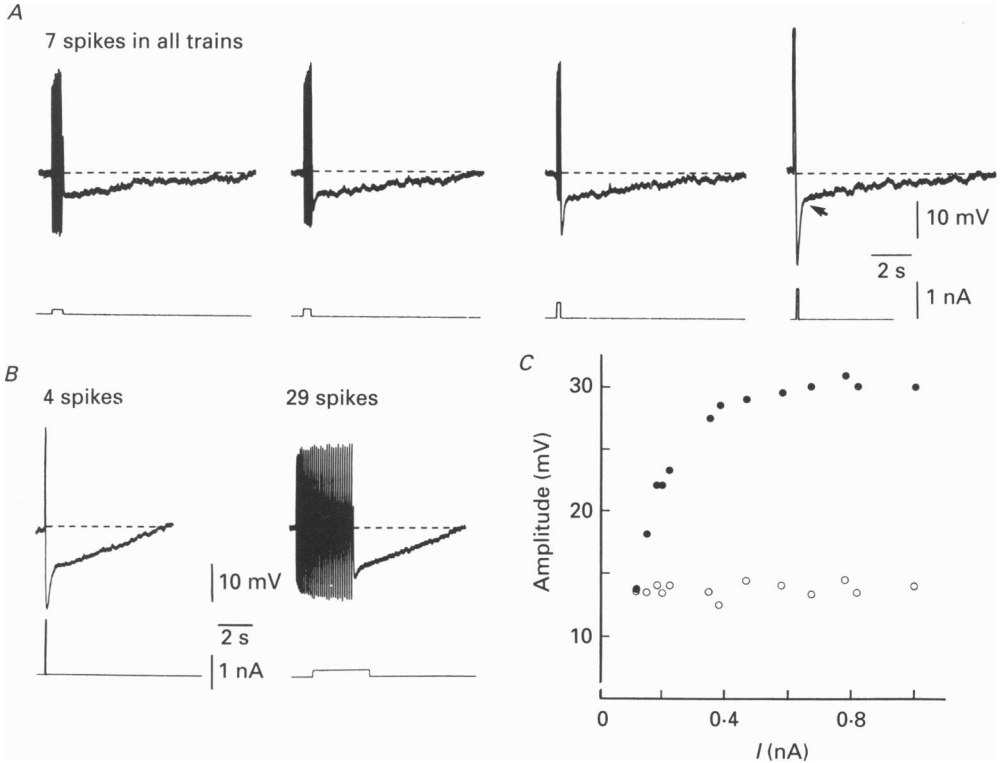
Fig. 1. Post-stimulus hyperpolarization (PSH) in LC neurons and dependence on stimulus intensity. *A*, chart records of four PSHs which follow a train of 7 spikes elicited with depolarizing current pulses of different intensities. Duration of the pulse was varied to keep the number of spikes in all trains the same. Upper trace is voltage and lower trace is current. Arrow on the PSH record (far right) represents the point where the amplitude of PSH_L was measured. Dashed lines represent the resting membrane potential. In this and all subsequent figures, spike amplitude is attenuated by the limited frequency response of the pen recorder. Membrane potential was -58 mV. *B*, an adequate intensity of the current stimulus is required to elicit PSH_E, regardless of the number of spikes in the train. Left, PSH following a train of 4 spikes, elicited with a short current pulse of high intensity, shows prominent PSH_E. Right, PSH following a train of 29 spikes, elicited with a longer pulse of low intensity. Upper trace is voltage and lower trace is current. Note that PSH following the train with 4 spikes elicited with the larger current pulse shows a prominent PSH_E, in contrast to the PSH following the train with 29 spikes elicited with a smaller current pulse. Membrane potential was -60 mV. *C*, dependence of the amplitude of PSH_E and PSH_L on the intensity of the current pulse used to elicit the action potential train in a typical LC neurone. Trains of 13 action potentials were elicited with depolarizing pulses of different current intensities; duration of the pulse was varied to keep the number of spikes in all trains the same. The PSH peak amplitude (●) and the amplitude of PSH_L (○) were measured (as described in text) and plotted as a function of intensity of the depolarizing pulse. Note that the peak amplitude of PSH is strongly dependent on the intensity of the current pulse, while the amplitude of PSH_L is not. Membrane potential was -60 mV. Different cells in *A*, *B*, and *C*.

PSH consists of two components

Previous studies (Andrade & Aghajanian, 1984; Williams *et al.* 1984) described a slow, prolonged hyperpolarization in LC neurons following a train of action

potentials. We report here that this hyperpolarization, which we call the post-stimulus hyperpolarization (PSH), is composed of two kinetically and pharmacologically distinct components. In the present study, trains of action potentials were evoked by injection of a depolarizing current pulse through the recording
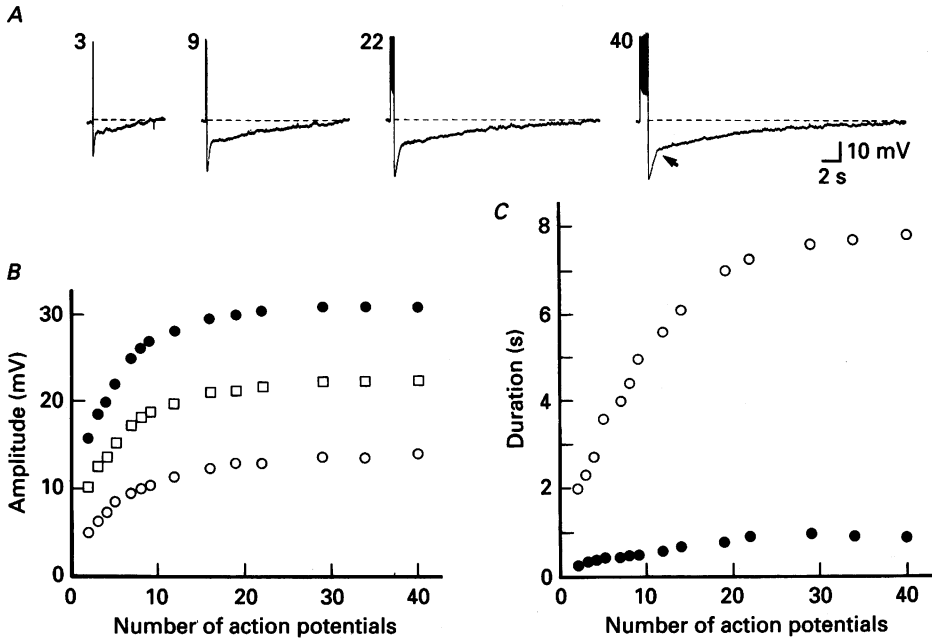

Fig. 2. Relation between the amplitude and duration of PSH_E and PSH_L and number of spikes in the train. A, chart records of several PSHs following trains of action potentials elicited with depolarizing current pulses, each of $1·1$ nA but of variable duration. The number of action potentials is shown at the top of each train. The intensity of the current stimulus was adequate to elicit PSH_E. Note that both PSH_E and PSH_L were augmented by increasing the number of action potentials in the train. Membrane potential was -59 mV. B, PSH peak amplitude ($\bullet$) and amplitude of PSH_L ($\bigcirc$) from the same experiment as in A are plotted as a function of the number of action potentials in the train. Amplitude of PSH_L was measured at the point shown by the arrow in A. $\square$, the amplitude of PSH_E estimated by subtracting the amplitude of PSH_L from the PSH peak amplitude. C, duration of PSH_E ($\bullet$) and half-duration of PSH_L ($\bigcirc$) are plotted as a function of the number of action potentials in the train. Duration of PSH_E was measured as the time from the peak amplitude of PSH to the appearance of PSH_L. Half-duration of PSH_L was measured from the beginning of PSH_L until decay to half-amplitude. Note that the time course of PSH_L shows a much larger dependence on the number of spikes in the train than does the time course of PSH_E.

electrode and PSH following the trains was measured. The experiment shown in Fig. 1 illustrates how PSH changes as a function of stimulus intensity. Figure 1A shows PSH elicited with depolarizing current pulses of different intensities; the number of spikes in the trains was kept constant (at 7) by decreasing the duration of the pulse as stimulus intensity was increased. Note that the PSH elicited by the smallest stimulus pulse was slow and monophasic (far left trace). When the stimulus intensity was sufficiently high, an additional faster phase of PSH appeared immediately

following the train. The amplitude of this fast, early phase (PSH_E) increased with increasing intensity of the current stimulus. Note that the slow, late phase (PSH_L) was of similar size and duration after all the trains.

Figure 1B illustrates that stimulus intensity is a more important determinant of the amplitude of PSH_E, than is the number of spikes in the train. A brief, large-amplitude stimulus pulse which evokes only four spikes is followed by a large early component of PSH, whereas a longer duration stimulus of lower amplitude evokes twenty-nine spikes, but only a very small PSH_E.

Figure 1C shows graphically how PSH_E changes as a function of stimulus current amplitude, whereas the late PSH_L does not. In this experiment, test trains were evoked at thirteen different current intensities. The duration of the current pulses was adjusted so that each train consisted of thirteen action potentials. The amplitude of PSH_E and PSH_L were plotted *versus* current intensity. As long as the number of spikes in the train remains the same, the slow component of PSH remains virtually unchanged, regardless of the amplitude of the current pulse. By contrast, PSH_E amplitude is strongly dependent on the intensity of the depolarizing current pulse, increasing as a function of current intensity. Qualitatively similar data were obtained in five other LC neurons.

From these experiments, it is apparent that the depolarizing current stimulus must exceed some threshold intensity in order to elicit PSH_E. Above this threshold value, PSH_E increases as a function of stimulus intensity. In most LC neurons in this study, PSH_E reached near-maximal amplitudes with depolarizing pulses of 0·4–0·6 nA. In view of this, for all subsequent experiments, we elicited trains of action potentials with depolarizing current pulses of sufficient intensity to evoke PSH_E.

Previous experiments have shown that the amplitude and duration of PSH increased with increasing number of action potentials in the train (Andrade & Aghajanian, 1984). In the present experiments, we tested the effect of number of action potentials in the train on the amplitude and time course of PSH_E and PSH_L using a stimulus intensity which was adequate to evoke PSH_E. The number of action potentials in the train was increased by prolonging the duration of the stimulus pulse. Figure 2A illustrates a typical example of the augmentation of both components with increasing number of action potentials in the train. This is further illustrated on the graph in Fig. 2B; note that in this LC neuron, both PSH_E and PSH_L approached their maximal amplitudes after twelve spikes. The graph in Fig. 2C shows that an increase in the number of action potentials in the train caused a large increase in the duration of PSH_L while only a slight prolongation of PSH_E.

In order to compare the amplitude and duration of PSH components among different LC neurons, we elicited a standard train of seven action potentials with depolarizing pulses 100 ms in duration. The intensity of the current was adjusted for each cell to obtain a train of seven action potentials. In sixteen LC neurons, the peak amplitude of PSH following such trains was $25·4 \pm 0·7$ mV (mean $\pm$ S.E.M.) and the amplitude of PSH_L was $9·1 \pm 0·4$ mV. The PSH_E amplitude, as estimated by subtraction of the PSH_L amplitude from the peak amplitude of PSH in each cell, was $16·3 \pm 0·5$ mV. The duration of PSH_L was 9800 ± 530 ms and the duration of PSH_E, measured at the point of merging with PSH_L, was 541 ± 31 ms.

Both PSH_E and PSH_L were associated with a decrease in membrane resistance

(Fig. 3*A*). Since hyperpolarization of LC neurons may decrease the input resistance due to activation of inward rectification (Osmanović & Shefner, 1987), we measured the changes in input resistance during PSH after blocking inward rectification with external Cs^+. In all five LC neurons tested, the extent of resistance changes during

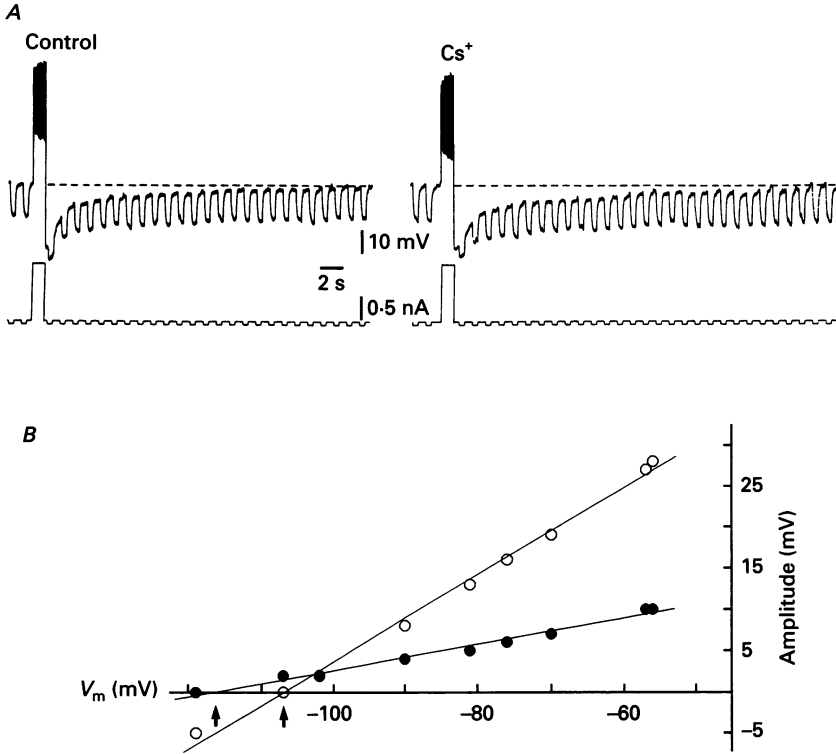Fig. 3. Changes in input resistance during PSH and determination of reversal potentials for PSH_E and PSH_L. *A*, PSH was elicited with a 500 ms depolarizing pulse in control ACSF (left) and 10 min after external application of 2 mM Cs^+ (right). Upper trace is voltage and lower trace is current. Input resistance was measured by passing constant hyperpolarizing current pulses and recording the corresponding voltage responses (upper trace). Note that a decrease in input resistance occurs during both phases of PSH and persists after block of inward rectification with Cs^+. Membrane potential was -58 mV and was unchanged by Cs^+. *B*, reversal potential for PSH_E and PSH_L. PSH was elicited with a 300 ms depolarizing pulse of 0.4 nA, at different membrane potentials (V_m). Peak amplitude of PSH (●), which represents PSH_E, and the amplitude of PSH_L, taken 1000 ms after the end of train (○), are plotted as a function of the membrane potential. Lines were drawn by linear regression. Arrows mark the reversal potential for two PSH components. Note that PSH_E reverses at -107 mV while the estimated reversal potential for PSH_L was -116 mV. Membrane potential was -57 mV. Different cells in *A* and *B*.

both phases of PSH was similar before and after addition of 2 mM Cs^+. Cs^+ slightly augmented both PSH components, probably by increasing the amplitude and duration of individual action potentials during the train (not shown).

The reversal potential for PSH_E and PSH_L was estimated by the method depicted in Fig. 3*B*. The amplitude of each of the two components was plotted as a function of membrane potential and the reversal potential was measured from the intersection

of the membrane potential axis and the regression lines. The reversal potentials for PSH_E and PSH_L, estimated by this method, were $-108\cdot4\pm2\cdot1$ and $-114\cdot0\pm2\cdot4$ mV ($n = 9$), respectively.

The membrane currents underlying PSH could be demonstrated by switching to voltage-clamp mode immediately following the train of action potentials and holding the membrane potential at different levels. This procedure, referred to as a hybrid clamp (Pennefather, Lancaster, Adams & Nicoll, 1985), revealed the current flowing during both phases of PSH. A typical experiment with hybrid clamp is shown on the inset in Fig. 4A. The outward current tail which follows the train of action potentials contained an early, rapidly decaying component, I_E, followed by a late, slower decaying component, I_L. The time course of I_{PSH} decay could be fitted by a biexponential function of the form:

$$I_{PSH} = I_E \exp(-t/\tau_E) + I_L \exp(-t/\tau_L),$$

where τ_E and τ_L are time constants for the early and the late components of I_{PSH}, respectively.

In the experiment shown in Fig. 4A, τ_E and τ_L were 86 and 2400 ms, respectively. Time constants were determined in twelve LC neurons and τ_L was found to be, on average, $32\cdot6\pm3\cdot7$ times larger than τ_E.

Both I_E and I_L reverse polarity at hyperpolarized membrane potentials (Fig. 4B). To determine the reversal potential for I_E and I_L, trains of action potentials were elicited from resting membrane potentials and the holding potential after the train was stepped to different levels. The inset of Fig. 4B shows an example of I_{PSH} recorded at three different membrane potentials. At -58 mV (top trace) I_{PSH} was outward and there was a clear reversal at -121 mV (bottom trace). The graph in Fig. 4B shows a plot of amplitudes of I_E and I_L *versus* after-train membrane potential, taken from the same LC neuron. The amplitude of I_E was measured 50 ms after the train and the amplitude of I_L was measured 600 ms after the train, when the decay of I_E should be complete (> 5 time constants). The reversal potentials for I_E and I_L were determined from the intersection of the regression lines fitted to the data points with the zero current level. In six LC neurons, the reversal potentials for I_E and I_L determined by this method were $-107\cdot2\pm1\cdot5$ and $-112\cdot1\pm1\cdot8$ mV, respectively.

The reversal potentials for I_E and I_L were shifted to more positive potentials when the K^+ concentration in the ACSF was increased. The graphs in Fig. 4C and 4D show the relationship between the reversal potential for I_E and I_L and the external K^+ concentration. The slopes of the regression lines were 57·1 (C) and 57·6 mV (D) per ten-fold increase in K^+ concentration. These values are close to the theoretical value predicted by the Nernst equation for a pure K^+ conductance (61·3 mV per tenfold change in $[K^+]_o$ at 36 °C) which indicates that both I_E and I_L are K^+ currents.

Ca²⁺ dependence of PSH

When the ACSF superfusing the preparation was changed to a solution containing zero Ca^{2+}, both PSH components were reduced ($n = 4$). Superfusion with Ca^{2+}-free ACSF caused marked membrane depolarization, reduced input resistance, changes in spontaneous firing and deterioration of the condition of the cell. To avoid these changes, the Ca^{2+} dependence of PSH was tested with ACSF containing 0·25 Ca^{2+} and
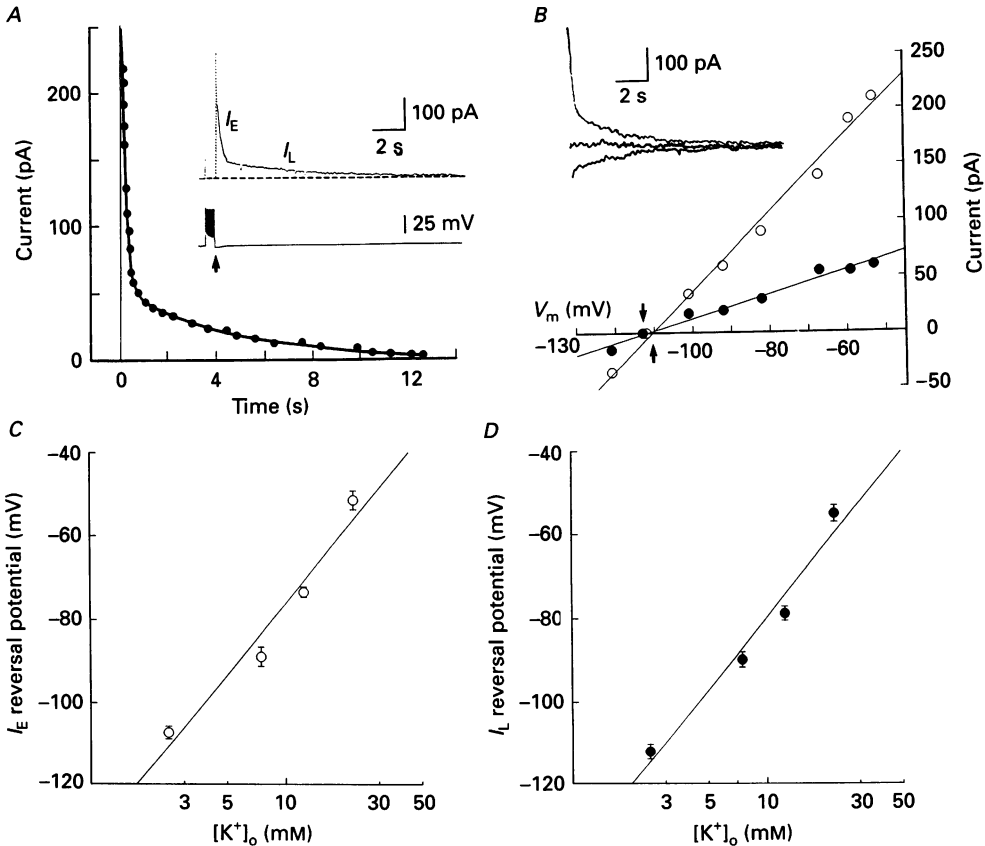
Fig. 4. The membrane currents underlying PSH and dependence on external K⁺ concentration. *A*, the inset was recorded during a 'hybrid clamp' experiment showing the outward current which underlies PSH; lower trace is voltage and upper trace is current. Immediately after the train of 15 action potentials (arrow) the circuit was switched to voltage clamp mode. Note that the outward tail current has a fast and slow component corresponding to PSH_E and PSH_L, respectively. The dashed line indicates the zero current level at the resting membrane potential of -59 mV. The graph shows the time course of the outward current underlying PSH. Filled circles are data points and the line was fitted with a biexponential function as described in text. Time constants of decay were 86 and 2400 ms, for the early and late current components, respectively. *B*, determination of the reversal potential for I_E and I_L. Trains of 8 action potentials were elicited from the resting membrane potential and the after-train potential (V_m) was clamped at different levels. Reversal potentials were determined by plotting the amplitude of the current at 50 ms (for I_E) and 600 ms (for I_L) after the train, as a function of after-train holding potential. $\bigcirc$, I_E; $\bullet$, I_L. The continuous lines were fitted to the data points by the least-squares method. Positive values correspond to the outward and negative values to the inward current. Upward and downward arrows mark the reversal potentials for I_E and I_L, respectively. Inset shows three current tails from the same neuron at, from top to bottom, -58, -112 and -121 mV. Different cells in *A* and *B*. *C* and *D*, relationship between the reversal potential for I_E and I_L and external K⁺ concentration. Graphs represent reversal potentials of I_E (*C*) and I_L (*D*) measured in ACSF of varying K⁺ concentrations. Reversal potentials were determined from the plots of current amplitude *versus* membrane potential as shown in *B*. Each point on the graph is the mean reversal potential ± S.E.M. for at least three LC neurons. The continuous lines were fitted to the data points by the least-squares method and have slopes of 57·1 (*C*) and 57·6 mV (*D*) per tenfold change in external K⁺ concentration.

20 mM Mg^{2+}. In four cells tested, this solution reversibly reduced both components of PSH (Fig. 5A). It was noted, however, that PSH_E was blocked much more quickly than PSH_L. It was necessary to superfuse with low-Ca^{2+}, high-Mg^{2+} ACSF for 20–30 min to substantially reduce PSH_L, and some residual hyperpolarization could still be seen at depolarized membrane potentials.
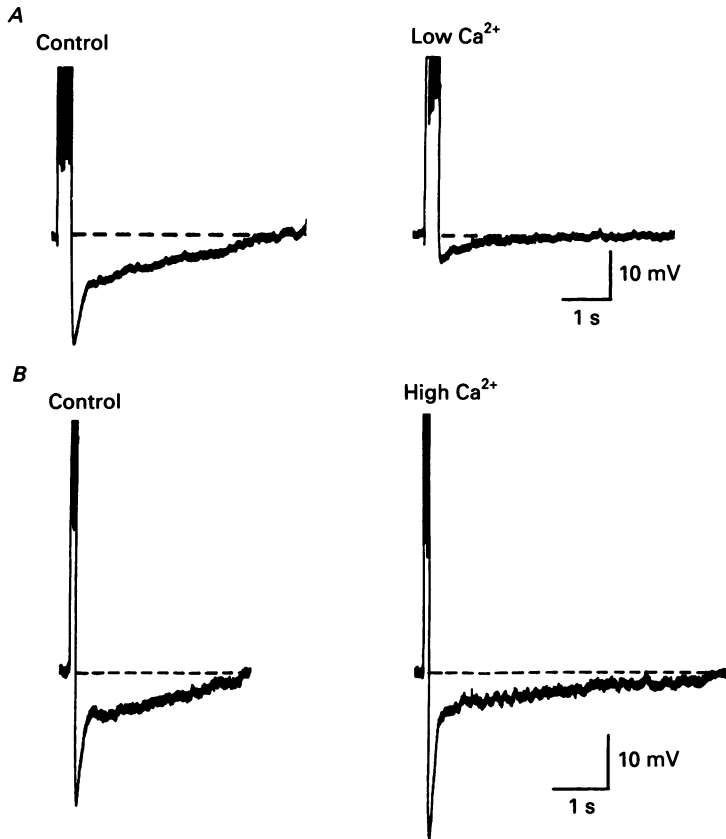

Fig. 5. Dependence of PSH on external Ca^{2+} concentration. A, PSH elicited with a 300 ms depolarizing pulse of 0·5 nA in control, and after 7 min of superfusion with ACSF containing 0·25 mM Ca^{2+} and 20 mM Mg^{2+}. Note the block of both PSH_E and PSH_L in low-Ca^{2+}, high-Mg^{2+} media. Membrane potential was -58 mV in control and was clamped back to the same value from -48 mV in low Ca^{2+}. B, PSH elicited with a 200 ms depolarizing pulse of 0·6 nA in control ACSF (2·5 mM Ca^{2+}) and after 10 min of superfusion with ACSF containing 6·5 mM Ca^{2+}. Note the increase in the amplitude of PSH_E and the prolongation of PSH_L in high-Ca^{2+} media. Membrane potential was -60 mV in control and -62 mV in high Ca^{2+}. Different cells in A and B.

The Ca^{2+} dependence of PSH was further tested by increasing the Ca^{2+} concentration in the ACSF. In three LC neurons tested, raising the Ca^{2+} concentration from 2·5 to 6·5 mM increased the amplitude of PSH_E and the duration of PSH_L (Fig. 5B). This effect was accompanied by inhibition of spontaneous firing and an enhancement of accommodation during the train (not shown).

Additional evidence for the Ca^{2+} dependence of PSH was obtained in experiments with Ca^{2+} channel blockers. Bath application of Cd^{2+} (200–500 μM) reversibly inhibited both components of PSH in all six cells tested. Figure 6A shows a typical example in which 500 μM Cd^{2+} greatly reduced both PSH_E and PSH_L evoked with a
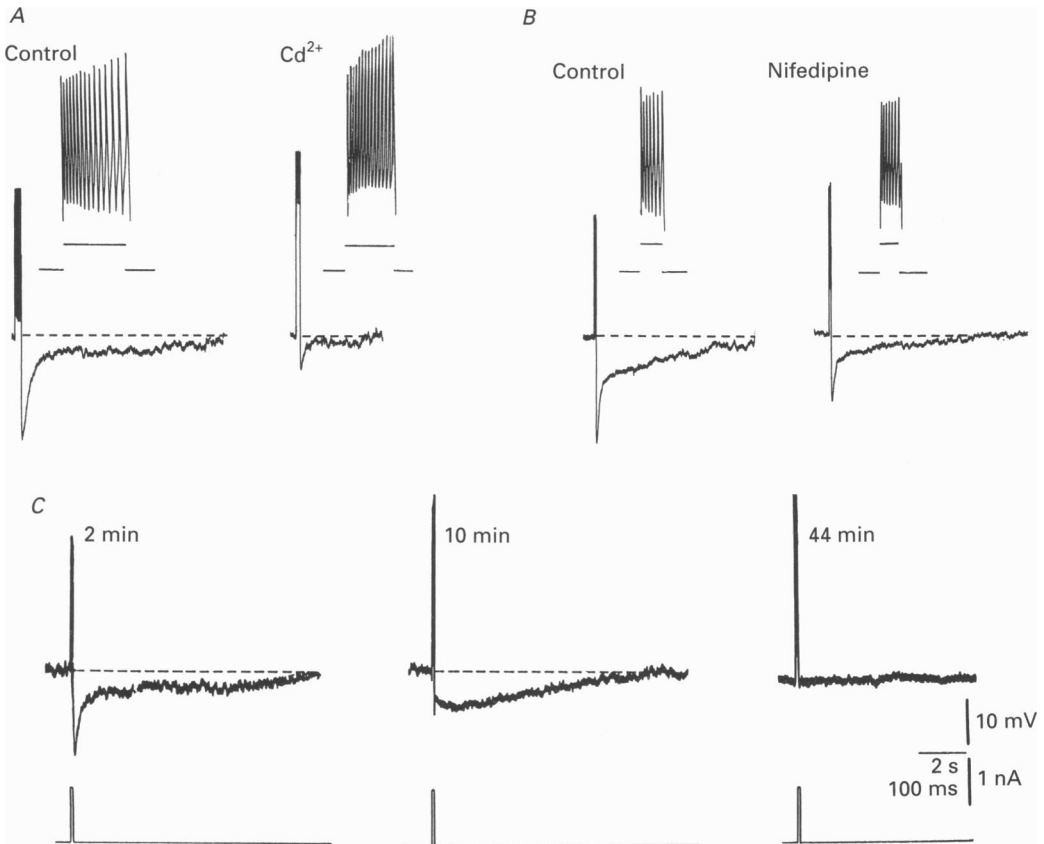

Fig. 6. Effects of Ca^{2+} channel blockers and intracellular EGTA on PSH. A, PSH following a train of 15 spikes in control, and after 17 min of superfusion with ACSF containing 500 μM Cd^{2+}. In this and subsequent figures insets show chart records, on an expanded time scale, of depolarizing pulses (lower traces) and trains of action potentials (upper traces) which were used to elicit PSH. To obtain the same number of action potentials in the train, the duration of the depolarizing pulse was decreased in Cd^{2+}. Note the complete block of both components of PSH by Cd^{2+}. Membrane potential was -59 mV and was clamped back to that value from -53 mV in Cd^{2+}. B, PSH elicited with a train of 7 spikes in control ACSF, and after 15 min of superfusion with ACSF containing 30 μM nifedipine. To obtain the same number of action potentials in the train, the duration of the depolarizing pulse was decreased slightly in nifedipine. Note that nifedipine reduced both components of PSH. Membrane potential was -59 mV and was unchanged by nifedipine. Different cells in A and B. C, effect of intracellular EGTA on PSH. PSH following a train of 6 spikes: 2 (left), 10 (middle) and 44 min (right) after impalement of a LC neuron with a microelectrode filled with 0·5 mM EGTA in 4 M potassium acetate. Upper trace is voltage and lower trace is current. Note that PSH_E was blocked by EGTA much sooner than PSH_L. Membrane potential was -59 mV. Calibration bars in C also apply to A and B.

train of fifteen action potentials. Furthermore, superfusion with nifedipine, an organic blocker of L-type Ca^{2+} channels, reduced, but did not abolish, both components of PSH in three LC neurons tested (Fig. 6B). In two LC neurons, superfusion of ACSF containing 500 μM of Ni^{2+}, a blocker of T-type Ca^{2+} channels, did not alter PSH (not shown).
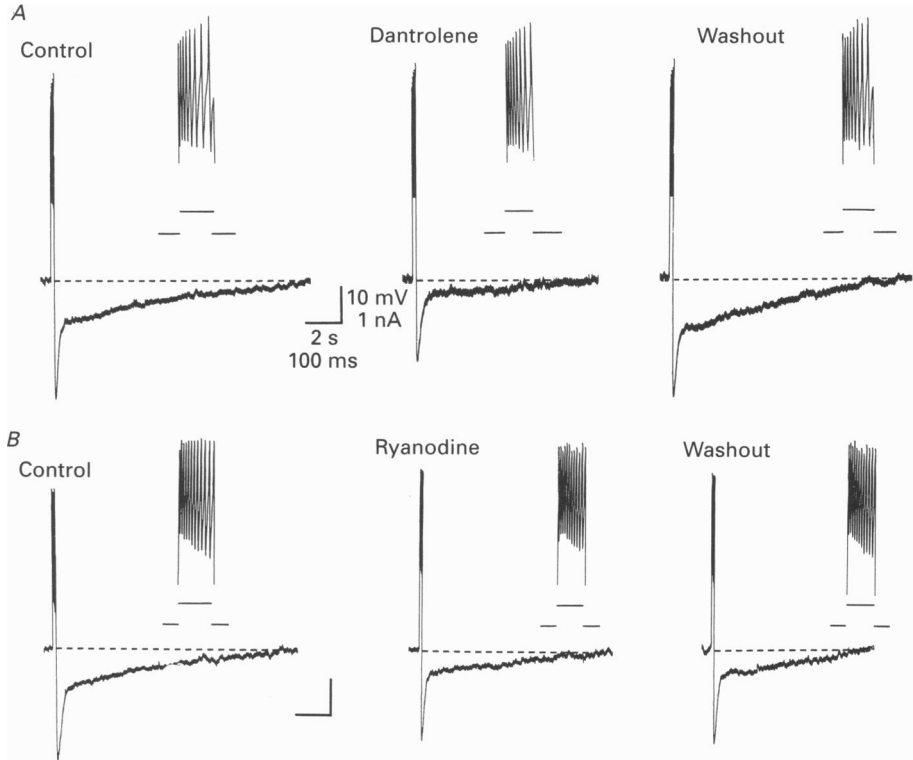

Fig. 7. Effects of dantrolene and ryanodine on PSH. A, PSH following a train of 8 spikes in control, after 25 min of perfusion with 25 μM dantrolene, and 15 min after washout of dantrolene. Note that dantrolene markedly reduced PSH_L. PSH_E as estimated by subtraction of PSH_L amplitude from peak PSH showed very little change. Also note the rebound enhancement of PSH_L after washout. Membrane potential was -58 mV and was unchanged by dantrolene. B, PSH following a train of 12 action potentials in control, after 30 min of perfusion with 20 μM ryanodine, and 35 min after washout of ryanodine. Note the selective inhibition of PSH_L by ryanodine and the poor reversibility of this effect upon washout. Membrane potential was -60 mV and was unchanged by ryanodine. Different cells in A and B.

The Ca^{2+} dependence of PSH was also tested by intracellular injection of the Ca^{2+} chelator, EGTA, in three LC neurons. Figure 6C shows that PSH_E was quickly and completely blocked several minutes after impalement with an EGTA-containing electrode. PSH_L was also inhibited by EGTA, but this occurred more slowly; about 40 min was required to fully abolish PSH_L. The finding that PSH_E was clearly more sensitive to the blocking effect of EGTA than PSH_L was also observed in the two other cells tested.
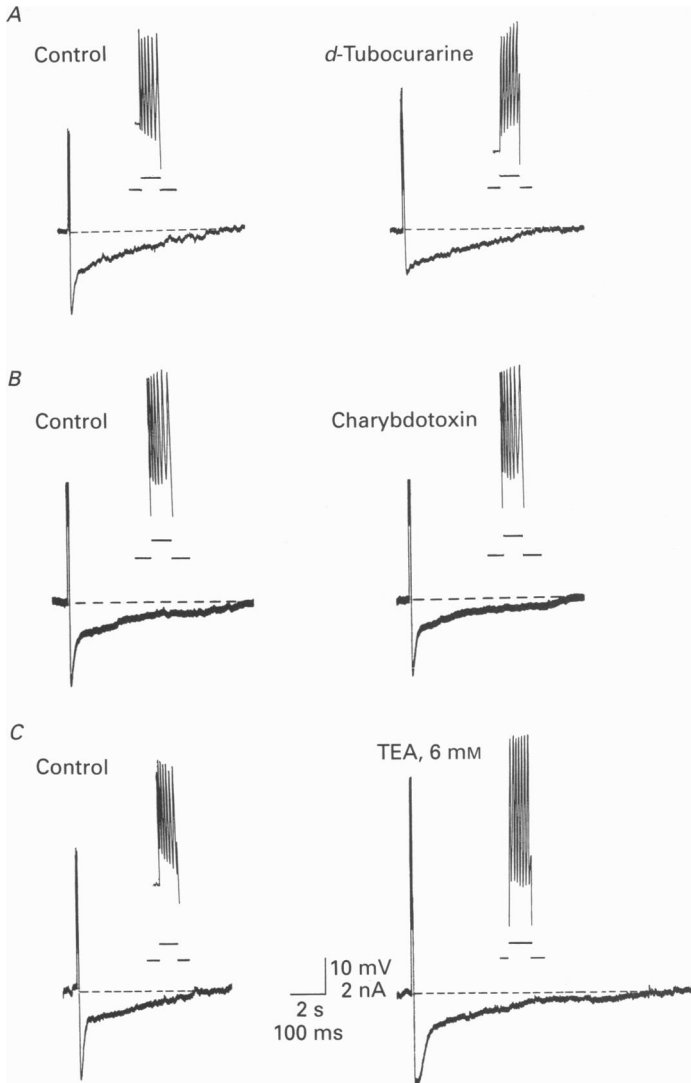
Fig. 8. Effects of *d*-tubocurarine, charybdotoxin and TEA on PSH. *A*, PSH following a train of 6 spikes in control and 8 min after addition of 100 μM *d*-tubocurarine (dTC). Note the selective block of PSH$_E$ by dTC. Membrane potential was −59 mV in control and was unchanged by dTC. *B*, effect of charybdotoxin (CTX). PSH following a train of 7 spikes in control and after 20 min of superfusion with 45 nM CTX. Note a lack of the effect of CTX on PSH. Membrane potential was −60 mV and was not changed by CTX. *C*, effects of a higher concentration of TEA on PSH. PSH following a train of 7 spikes in control and after 10 min of superfusion with 6 mM TEA To obtain the same number of spikes in the train, the duration of the current pulse was slightly increased in TEA. Note that at this concentration TEA increased the duration of both PSH$_E$ and PSH$_L$. Membrane potential was −59 mV and was clamped back to that value from −61 mV in TEA. Different cells in *A*, *B* and *C*. Calibration bars in *C* also apply to *A* and *B*.

Neurons have intracellular stores of Ca^{2+} which can be released by Ca^{2+} influx during action potentials; such release can be blocked by several agents including dantrolene and ryanodine (see Henzi & MacDermott, 1992, for review). Such Ca^{2+}-induced Ca^{2+} release from intracellular stores has been reported to contribute to the generation of prolonged after-hyperpolarizations in other preparations (Kawai & Watanabe, 1989; Sah & McLachlan, 1991). Dantrolene and ryanodine were used to test the possible involvement of Ca^{2+}-induced Ca^{2+} release in the generation of PSH in LC neurons. Figure 7A shows that dantrolene inhibited PSH_L with less effect on PSH_E. In four neurons superfused with 25 μM dantrolene, the amplitude of PSH_L was reduced by $36\cdot6\pm5\cdot2\%$ and the duration of PSH_L was reduced by $26\cdot3\pm5\cdot0\%$; the amplitude of PSH_E was decreased by $10\cdot2\pm4\cdot3\%$, but with no change in duration. The effects of dantrolene were fully reversible upon washout and there was usually a rebound increase in the size of PSH_L after washout. Ryanodine caused a similar inhibition of PSH_L with little change in PSH_E (Fig. 7B). Superfusion of ryanodine (20 μM) decreased the amplitude and duration of PSH_L by $31\cdot3\pm3\cdot7$ and $31\cdot2\pm3\cdot8\%$, respectively ($n = 6$). The amplitude of PSH_E was decreased by only $4\cdot3\pm1\cdot7\%$, with no change in duration. In contrast to dantrolene, the effects of ryanodine were slow in onset and poorly reversible upon washout. Both ryanodine and dantrolene also decreased the accommodation of firing during spike trains (insets on Fig. 7), suggesting that PSH_L may contribute to the accommodation of firing seen in these neurons.

Effects of d-tubocurarine

Slow after-hyperpolarizations in many preparations have been shown to be mediated by small-conductance Ca^{2+}-activated K^+ channels (SK channels), which can be blocked by apamin (Blatz & Magleby, 1986). We have previously reported that in LC neurons apamin selectively abolishes PSH_E (Osmanović, Shefner & Brodie, 1990). d-Tubocurarine (dTC) has also been shown to inhibit slow after-hyperpolarizations in several preparations (Nohmi & Kuba, 1984; Bourque & Brown, 1987), probably by blocking SK channels (Cook & Haylett, 1985). The effect of dTC on PSH was tested in twelve LC neurons. A typical example is shown in Fig. 8A. In two cells, 20 μM dTC selectively decreased the amplitude of PSH_E. In seven other LC neurons, 100–200 μM dTC completely abolished PSH_E with no effect on the PSH_L. This effect was accompanied by the same changes in the single spike after-hyperpolarization and accommodation as those of apamin (see Osmanović *et al.* 1990). In contrast to apamin, these effects of dTC were fully reversible with washout.

Effects of I_c antagonists

We examined the possibility that a portion of PSH could be due to activation of the fast, Ca^{2+}-activated K^+ current, I_c (Adams, Constanti, Brown & Clark, 1982), which is mediated by large-conductance Ca^{2+}-activated K^+ channels (BK channels). Charybdotoxin (CTX) is a potent blocker of BK channels (Miller, Moczydlowski, Latorre & Phillips, 1985). In three LC neurons, 40 nM CTX did not inhibit either component of PSH (Fig. 8B).

At submillimolar doses, TEA has been shown to be a rather specific antagonist of I_c in vertebrate neurons (Adams *et al.* 1982; Lancaster & Nicoll, 1987; Storm, 1987).

We tested the effects of low concentrations of TEA (400 μM–1 mM) on five LC neurons. TEA prolonged PSH_L with little change in PSH_E (data not shown). If the number of spikes in the train was kept the same as in control, TEA increased the duration of PSH_L by $45 \pm 17\%$ ($n = 5$). The amplitude of PSH_L was unchanged in two cells and increased in three cells (by $16 \pm 1\%$). This enhancement of PSH_L was probably secondary to increased Ca^{2+} influx during the train, due to the broadening of action potentials by TEA (not shown).

Effects of higher concentrations of TEA and 4-AP

TEA at higher concentrations is known to block a variety of K^+ channels, in addition to the BK channels. The effect of higher concentrations of TEA (2–10 mM) on PSH was tested in nine LC neurons. In this concentration range, TEA caused a large increase in action potential duration. TEA-induced changes in PSH depended on the intensity of the depolarizing pulse used to elicit the train. As shown in Fig. 8C, if the intensity of the depolarizing stimulus was low, TEA caused a clear prolongation of both PSH_E and PSH_L in all cells tested. The mean increase in duration of PSH_E and PSH_L was 87.2 ± 26.4 and $107.6 \pm 18.4\%$, respectively. The amplitude of PSH_E was decreased in six of nine neurons (by $17.6 \pm 4.8\%$). In contrast, the amplitude of PSH_L was increased in five out of nine cells (by $36.3 \pm 22.5\%$). When higher intensity stimuli were used to evoke the trains, changes in PSH were difficult to interpret due to the concomitant development of an after-depolarization (ADP) with a time course which overlapped with PSH.

A fast, transient K^+ current, I_A has been demonstrated in LC neurons (Williams *et al.* 1984) and could contribute to PSH in these neurons. The possible role of I_A in the generation of PSH was tested by application of 4-aminopyridine (4-AP) or diaminopyridine (DAP), agents which block this current. In four neurons tested, these drugs enhanced PSH_L with less effect on PSH_E (Fig. 9A). This effect was probably secondary to the increase in amplitude and duration of action potentials caused by these agents (see inset on Fig. 9A).

Neurotransmitter modulation of PSH

Noradrenaline (NA) has been shown to inhibit slow after-hyperpolarizations in several preparations by acting via β-adrenergic receptors to increase cAMP (Madison & Nicoll, 1982, 1986; Schwindt, Spain, Foehring, Chubb & Crill, 1988a). Effects of NA (10 μM) on PSH were tested in three LC neurons. NA application caused membrane hyperpolarization, as previously reported (Williams, Henderson & North, 1985); if PSH was elicited during the NA-induced hyperpolarization both components were decreased in size. If the membrane potential was clamped back to the control value and the same action potential train was elicited, however, PSH was unchanged (data not shown).

The effect of increased intracellular cAMP on PSH was tested by superfusing the slice with membrane-permeable analogues of cAMP, dibutryl cAMP and 8-Br-cAMP. Prolonged superfusion (20–40 min) with these agents at a concentration of 1 mM, caused a small depolarization and an increase in the spontaneous firing rate, as previously reported (Wang & Aghajanian, 1987), but did not affect PSH in any of the five LC neurons tested (data not shown). The action of some other agents which have

been shown to modulate Ca^{2+}-activated K^+ conductances by changing the level of intracellular cAMP in other preparations were also tested; histamine (100 μM; $n = 2$), adenosine (100 μM; $n = 3$) and serotonin (100 μM; $n = 2$) had no effect on PSH in LC neurons.
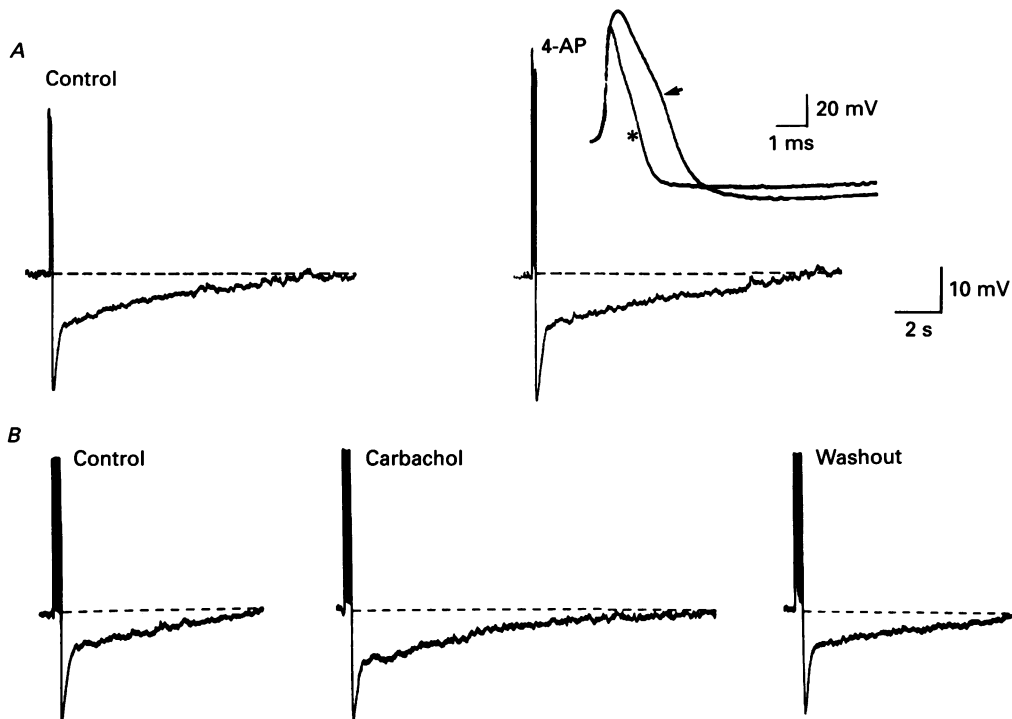

Fig. 9. Effects of 4-AP and carbachol on PSH. A, PSH following a train of 6 spikes in control ACSF and after 10 min of superfusion with 500 μM 4-AP. Note that 4-AP clearly enhanced PSH_L and only slightly increased PSH_E. The inset shows the spontaneous action potential in control ACSF (asterisk) and in 4-AP (arrow); note that action potential amplitude and duration were increased by 4-AP. Membrane potential was -59 mV and was unchanged by 4-AP. B, PSH following a train of 14 spikes elicited with a depolarizing pulse of 0·75 nA in control, after 7 min of superfusion with 40 μM carbachol, and after washout of carbachol. Note the increase in amplitude and duration of PSH_L with no change in PSH_E. Membrane potential was -58 mV in control and was clamped back to this value from -54 mV in carbachol. Different cells in A and B.

ACh and muscarinic agonists strongly suppress Ca^{2+}-dependent after-hyper-polarizations in several preparations (Benardo & Prince, 1982; Cole & Nicoll, 1983; Lancaster & Nicoll, 1987; Schwindt $et~al.$ 1988a). Figure 9B shows that carbachol has the opposite effect on PSH in LC neurons, strongly enhancing PSH_L. Both the amplitude and duration of PSH_L were increased by carbachol (40–100 μM) in four out of six cells tested. Enhancement of PSH_L by carbachol is probably not caused by increased Ca^{2+} influx during the train, since the number of spikes in the trains used to evoke PSH was kept constant and carbachol did not change the duration or amplitude of action potentials. The cholinergic enhancement was selective for PSH_L;

PSH_E was unaffected by carbachol. Preliminary experiments indicate that the effect of carbachol on PSH can be mimicked by muscarine and blocked by pirenzepine. A paper describing muscarinic modulation of PSH in LC neurons is in preparation.

<div align="center">DISCUSSION</div>

The results presented above indicate that PSH in LC neurons is mediated by two distinct Ca^{2+}-activated K^+ currents which have different pharmacological properties and physiological functions. One of these currents, I_E, is blocked by apamin and dTC, and is responsible for PSH_E, as well as the fast phase of accommodation of firing (see Osmanović *et al.* 1990). The other current, I_L, is apamin-resistant and has a slower time course of decay; it underlies PSH_L and may be responsible for the slow phase of accommodation of firing.

Our data indicate that both I_E and I_L are K^+ currents. Their reversal potentials are close to the value of E_K (potassium equilibrium potential) in control media and change with increases in external K^+ concentration according to the Nernst equation for pure K^+ currents. Several lines of evidence suggest that both PSH_E and PSH_L in LC neurons are mediated by Ca^{2+}-activated K^+ conductances: (a) both components depend on the number of action potentials in the train, (b) both components are reduced or abolished by decreasing the Ca^{2+} concentration in the bathing medium, (c) both components are inhibited by Ca^{2+} channel blockers, (d) both components are augmented by increased external Ca^{2+} concentration and (e) both components are inhibited by intracellular EGTA. It has been previously shown that more than one type of Ca^{2+}-activated K^+ conductance can contribute to after-hyperpolarizations within the same cell (Romey & Lazdunski, 1984; Pennefather *et al.* 1985; Lancaster & Adams, 1986; Lancaster & Nicoll, 1987; Lang & Ritchie, 1987; Schwindt, Spain, Foehring, Stafstrom, Chubb & Crill, 1988*b*; Sah & McLachlin, 1991). These after-hyperpolarizations vary widely in their size and duration, sensitivity to various K^+ channel blockers and susceptibility for modulation by different neurotransmitters. There is also a lack of consistent nomenclature for these after-hyperpolarizations in different preparations. Therefore, the following comparison of PSH in LC neurons to similar after-hyperpolarizations in other preparations is based on their pharmacological properties and time course.

PSH_E in LC neurons resembles the mAHP recorded in neocortical pyramidal neurons (Schwindt *et al.* 1988*b*) in that it is apamin sensitive and TEA resistant and has a similar time course and functional role in accommodation of firing. PSH_E also resembles the apamin-sensitive after-hyperpolarizations described in other central and peripheral neurons (Pennefather *et al.* 1985; Kawai & Watanabe, 1986; Sah & McLachlan, 1991). In the present study, we found that in addition to being apamin sensitive, PSH_E in LC neurons was also selectively blocked by dTC. This finding is consistent with previous reports that dTC inhibits apamin-sensitive after-hyperpolarizations in other preparations (Nohmi & Kuba, 1984; Bourque & Brown, 1987; Goh & Pennefather, 1987; Morita & Katayama, 1989). Interestingly, PSH_E in LC neurons can be elicited only if the depolarizing current pulse intensity exceeds a threshold value; to our knowledge, this property has not been previously reported for similar after-hyperpolarizations. As LC neurons in the slice have extensive dendrites,

technical limitations in controlling the voltage in distal dendrites hamper a more quantitative examination of the apparent threshold nature of this phenomenon. It is possible that activation of the conductance underlying PSH_E requires Ca^{2+} influx through high-threshold Ca^{2+} channels which are not activated by depolarizing current pulses of lower intensity. Alternatively, the PSH_E conductance may be localized, together with Ca^{2+} channels, on dendrites far from the current injection site in the soma. Another possibility is that this phenomenon could result simply from the intrinsic voltage dependence of the PSH_E conductance itself, which could require a stronger depolarization to be activated. This latter suggestion is unlikely, since single channel studies show that apamin-sensitive (SK) channels in other preparations show little voltage dependence (Blatz & Magleby, 1986; Lang & Ritchie, 1987).

PSH_L described in this study differs from PSH_E in several respects. The time course of decay of PSH_L is more than one order of magnitude slower than that of PSH_E. In addition, unlike PSH_E, PSH_L is resistant to apamin and dTC, but is reduced by dantrolene and ryanodine. Furthermore, PSH_L activation does not require a high-intensity depolarizing current pulse; it is evoked by any train of action potentials. PSH_L resembles slow after-hyperpolarizations in hippocampal pyramidal neurons (Lancaster & Adams, Lancaster & Nicoll, 1987) and in vagal motoneurons (Sah & McLachlin, 1991). Similarities include a slow time course, Ca^{2+} dependence, insensitivity to apamin and to low concentrations of external TEA. Furthermore, PSH_L can be reduced by blockers of Ca^{2+}-induced Ca^{2+} release from intracellular stores, as described previously for vagal motoneurons (Sah & McLachlin, 1991). PSH_L differs, however, from these after-hyperpolarizations in its susceptibility to modulation by neurotransmitters. In both hippocampal and vagal motorneurons, NA inhibits the current underlying the slow after-hyperpolarization, and this effect is mediated by β-adrenergic receptors. In our study NA did not affect PSH_L, which is consistent with the absence of β-adrenergic receptors on LC neurons. PSH_L, however, also was unaffected by membrane-permeable analogues of cAMP and neurotransmitters (adenosine, histamine, serotonin) which increase intracellular cAMP in many other preparations. It is well known that these agents are potent inhibitors of slow after-hyperpolarizations in hippocampal neurons (Madison & Nicoll, 1982; Lancaster & Nicoll, 1987). An additional finding in the present study was that PSH_L was strongly enhanced by carbachol. Muscarinic agonists have been shown to potently inhibit slow after-hyperpolarizations in hippocampal and other neurons (Cole & Nicoll, 1983; Lancaster & Nicoll, 1987; Schwindt et al. 1988a). To our knowledge, PSH_L in LC neurons is the only example of an after-hyperpolarization in central neurons which is enhanced by muscarinic agonists.

A single channel study in hippocampal pyramidal neurons (Lancaster, Nicoll & Perkel, 1991) has revealed a distinct population of Ca^{2+}-dependent K^+ channels, which, according to their pharmacological properties, may mediate the slow after-hyperpolarization in these cells. Single channel studies in LC neurons will be required to determine whether similar channels mediate PSH_L.

Although PSH_L is clearly dependent on Ca^{2+} entry during the spike train, it is more resistant than PSH_E to manipulations which affect Ca^{2+} influx. Specifically, PSH_L is inhibited more slowly and to a lesser extent by reduction of external Ca^{2+},

application of Ca^{2+} channel blockers and injection of intracellular EGTA than is PSH_E. Similarly, when external Ca^{2+} is raised, PSH_L shows less augmentation than PSH_E. These differences in the dependence on extracellular Ca^{2+} of the two components of PSH may be due to the fact that while both PSH_E and PSH_L are activated by the influx of Ca^{2+} during the train, the PSH_L conductance requires lower intracellular Ca^{2+} concentrations for activation. The prolonged time course of PSH_L, could then simply reflect the time course of Ca^{2+} removal from the Ca^{2+} binding site of the PSH_L conductance (i.e. Ca^{2+} buffering, sequestration or extrusion). Alternatively, the prolonged time course of PSH_L could be due to a prolonged, spatially restricted increase in intracellular Ca^{2+} in close proximity to PSH_L channels. Such an increase in intracellular Ca^{2+} may be caused by the release of Ca^{2+} from intracellular stores triggered by Ca^{2+} entry during the action potential train. Our data with dantrolene and ryanodine suggest that Ca^{2+}-induced Ca^{2+} release contributes to the generation of the PSH_L in LC neurons. A similar mechanism has been previously proposed to mediate a slow, apamin-resistant, Ca^{2+}-activated K^+ conductance ($G_{K_{Ca,2}}$) in vagal motoneurons (Sah & McLachlin, 1991).

In hippocampal pyramidal neurons (Lancaster & Nicoll, 1987) and sympathetic ganglion cells (Adams *et al.* 1982) a component of the hyperpolarization that follows a train of action potentials is mediated by the fast Ca^{2+}-activated K^+ current, I_c. I_c is thought to be carried by the large-conductance Ca^{2+}-activated K^+ channels (BK channels) which show strong voltage dependence and are highly sensitive to CTX and to low concentrations of external TEA. Our data indicate that neither PSH_E nor PSH_L in LC neurons are inhibited by external TEA in concentrations up to 1 mM or by CTX. This indicates that BK channels are not involved in generation of either PSH_E or PSH_L. I_c is known to deactivate rapidly at membrane potentials close to rest; this could explain why I_c doesn't contribute significantly to PSH_E and PSH_L, which have much slower kinetics.

In conclusion, the results of this study indicate that LC neurons have at least two different Ca^{2+}-activated K^+ conductances which are responsible for generation of distinct phases of the after-hyperpolarization following trains of spikes. One of these conductances is selectively blocked by apamin and dTC and mediates PSH_E. The other conductance, which is reduced by blockers of Ca^{2+}-induced Ca^{2+} release and enhanced by muscarinic agonists, mediates PSH_L. These two conductances would be expected to have distinct modulatory roles on excitability of LC neurons during the post-activation inhibitory period which follows high-frequency firing, *in vivo*. In addition, these conductances mediate accommodation of firing during action potential trains. We have previously shown that accommodation in LC neurons is a biphasic process with the apamin-sensitive conductance underlying the faster component (Osmanović *et al.* 1990). The present data suggest that the ryanodine-sensitive conductance may be the mechanism responsible for the slower component of accommodation.

REFERENCES

ADAMS, P. R., CONSTANTI, A., BROWN, D. A. & CLARK, R. B. (1982). Intracellular Ca^{2+} activates a fast voltage-sensitive K^+ current in vertebrate sympathetic neurones. *Nature* **296**, 746–749.

AGHAJANIAN, G. K., CEDARBAUM, J. M. & WANG, R. Y. (1977). Evidence for norepinephrine-mediated collateral inhibition of locus coeruleus neurons. *Brain Research* **136**, 570–577.

AGHAJANIAN, G. K. & VANDERMAELEN, C. P. (1982). α_2-Adrenoceptor-mediated hyperpolarization of locus coeruleus neurons: intracellular studies in vivo. *Science* **215**, 1394–1396.

AGHAJANIAN, G. K., VANDERMAELEN, C. P. & ANDRADE, R. (1983). Intracellular studies of the role of calcium in regulating the activity and reactivity of locus coeruleus neurons in vivo. *Brain Research* **273**, 237–243.

ANDRADE, R. & AGHAJANIAN, G. K. (1984). Locus coeruleus activity in vitro: intrinsic regulation by a calcium dependent potassium conductance but not α_2-adrenoceptors. *Journal of Neuroscience* **4**, 161–170.

BENARDO, L. S. & PRINCE, D. A. (1982). Cholinergic excitation of mammalian hippocampal pyramidal cells. *Brain Research* **249**, 315–331.

BLATZ, L. A. & MAGLEBY, K. L. (1986). Single apamin-blocked Ca^{2+}-activated K channels of small conductance in cultured rat skeletal muscle. *Nature* **323**, 718–720.

BOURQUE, C. W. & BROWN, D. A. (1987). Apamin and d-tubocurarine block the afterhyper-polarization of rat supraoptic neurosecretory neurons. *Neuroscience Letters* **82**, 185–190.

COLE, A. E. & NICOLL, R. A. (1983). Acetylcholine mediates a slow synaptic potential in hippocampal pyramidal cells. *Science* **221**, 1299–1301.

COOK, N. S. & HAYLETT, D. G. (1985). Effects of apamin, quinine and neuromuscular blockers on calcium-activated potassium channels in guinea-pig hepatocytes. *Journal of Physiology* **358**, 373–394.

GOH, J. W. & PENNEFATHER, P. S. (1987). Pharmacological and physiological properties of the after-hyperpolarization current of bull frog ganglion neurones. *Journal of Physiology* **394**, 315–330.

HENZI, V. & MACDERMOTT, A. B. (1992). Characteristics and function of Ca^{2+}- and inositol 1,4,5,-trisphosphate-releasable stores of Ca^{2+} in neurons. *Neuroscience* **46**, 251–273.

KAWAI, T. & WATANABE, M. (1986). Blockade of Ca-activated K conductance by apamin in rat sympathetic neurons. *British Journal of Pharmacology* **87**, 225–232.

KAWAI, T. & WATANABE, M. (1989). Effects of ryanodine on the spike after-hyperpolarization in sympathetic neurones of the rat superior cervical ganglion. *Pflügers Archiv* **413**, 470–475.

LANCASTER, B. & ADAMS, P. R. (1986). Calcium-dependent current generating the afterhyper-polarization of hippocampal neurons. *Journal of Neurophysiology* **55**, 1268–1282.

LANCASTER, B. & NICOLL, R. A. (1987). Properties of two calcium-activated hyperpolarizations in rat hippocampal neurones. *Journal of Physiology* **389**, 187–203.

LANCASTER, B., NICOLL, R. A. & PERKEL, D. J. (1991). Calcium activates two types of potassium channels in rat hippocampal neurons in culture. *Journal of Neuroscience* **11**, 23–30.

LANG, D. G. & RITCHIE, A. K. (1987). Large and small conductance calcium-activated potassium channels in the GH3 anterior pituitary cell line. *Pflügers Archiv* **410**, 614–622.

MADISON, D. V. & NICOLL, R. A. (1982). Noradrenaline blocks accommodation of pyramidal cell discharge in the hippocampus. *Nature* **299**, 636–638.

MADISON, D. V. & NICOLL, R. A. (1986). Actions of noradrenaline recorded intracellularly in CA1 pyramidal neurones in vitro. *Journal of Physiology* **372**, 221–224.

MILLER, C., MOCZYDLOWSKI, E., LATORRE, R. & PHILLIPS, M. (1985). Charybdotoxin, a protein inhibitor of single Ca^{2+}-activated K^+ channels from mammalian skeletal muscle. *Nature* **313**, 316–318.

MORITA, K. & KATAYAMA, Y. (1989). Calcium-dependent slow outward current in visceral primary afferent neurones of the rabbit. *Pflügers Archiv* **414**, 171–177.

NOHMI, M. & KUBA, K. (1984). ($\pm$)-Tubocurarine blocks the Ca^{2+}-dependent K^+-channel of the bullfrog sympathetic ganglion cells. *Brain Research* **301**, 146–148.

OSMANOVIĆ, S. S. & SHEFNER, S. A. (1987). Anomalous rectification in rat locus coeruleus neurons. *Brain Research* **417**, 161–166.

OSMANOVIĆ, S. S. & SHEFNER, S. A. (1988). Baclofen increases the potassium conductance of rat locus coeruleus neurons recorded in brain slice preparation. *Brain Research* **438**, 124–136.

OSMANOVIĆ, S. S. & SHEFNER, S. A. (1990*a*). Two calcium-activated potassium conductances generate the post-stimulus hyperpolarization in rat locus coeruleus neurons. *Society for Neuroscience Abstracts* **16**, 508.

OSMANOVIĆ, S. & SHEFNER, S. A. (1990*b*). γ-Aminobutyric acid responses in rat locus coeruleus neurones *in vitro*: a current-clamp and voltage-clamp study. *Journal of Physiology* **421**, 151–170.

OSMANOVIĆ, S., SHEFNER, S. & BRODIE, M. (1990). Functional significance of the apamin sensitive conductance in rat locus coeruleus neurons. *Brain Research* **530**, 283–289.

PENNEFATHER, P., LANCASTER, B., ADAMS, P. R. & NICOLL, R. A. (1985). Two distinct Ca-dependent K currents in bullfrog sympathetic ganglion cells. *Proceedings of the National Academy of Sciences of the USA* **82**, 3040–3044.

ROMEY, G. & LAZDUNSKI, M. (1984). The coexistence in rat muscle cells of two distinct classes of Ca^{2+}-dependent K channels with different pharmacological properties and different physiological functions. *Biochemical and Biophysical Research Communications* **118**, 669–674.

RUDY, B. (1988). Diversity and ubiquity of K channels. *Neuroscience* **25**, 729–749.

SAH, P. & McLACHLAN, E. M. (1991). Ca^{2+}-activated K^+ currents underlying the afterhyperpolarization in guinea pig vagal neurons: a role for Ca^{2+}-activated Ca^{2+} release. *Neuron* **7**, 257–264.

SCHWINDT, P. C., SPAIN, W., FOEHRING, R. C., CHUBB, M. C. & CRILL, W. E. (1988*a*). Slow conductances in neurons from cat sensorimotor cortex in vitro and their role in slow excitability changes. *Journal of Neurophysiology* **59**, 450–467.

SCHWINDT, P. C., SPAIN, W. J., FOEHRING, R. C., STAFSTROM, C. E., CHUBB, M. C. & CRILL, W. E. (1988*b*). Multiple potassium conductances and their functions in neurons from cat sensorimotor cortex in vitro. *Journal of Neurophysiology* **59**, 424–449.

STORM, J. F. (1987). Action potential repolarization and a fast after-hyperpolarization in rat hippocampal pyramidal cells. *Journal of Physiology* **385**, 733–759.

WANG, Y. Y. & AGHAJANIAN, G. K. (1987). Excitation of locus coeruleus neurons by an adenosine 3′,5′-cyclic monophosphate-activated inward current: extracellular and intracellular studies in rat brain slices. *Synapse* **1**, 481–487.

WATABE, K. & SATOH, T. (1979). Mechanism underlying prolonged inhibition of rat locus coeruleus neurons following anti- and orthodromic activation. *Brain Research* **165**, 343–347.

WILLIAMS, J. T., HENDERSON, G. & NORTH, R. A. (1985). Characterization of α_2-adrenoceptors which increase potassium conductance in rat locus coeruleus neurones. *Neuroscience* **14**, 95–101.

WILLIAMS, J. T., NORTH, R. A., SHEFNER, S. A., NISHI, S. & EGAN, T. M. (1984). Membrane properties of rat locus coeruleus neurones. *Neuroscience* **13**, 137–156.